

A Simple Model to Predicting Pore Pressure from Shear Wave Sensitivity Analysis

Oluwatosin John ROTIMI^{a*}, Efeoghene ENAWORU^a, Charles Y. ONUH^a and Olumide Peter SOWANDE^a

^aPetroleum Engineering Department, Covenant University, Ota, Nigeria

*E-mail: oluwatosin.rotimi@covenantuniversity.edu.ng

Abstract

A successful seismicity alongside core analysis provides data for subsurface structural mapping, definition of lithology, identification of the productive zones, description of their depths and thickness. Inadequate understanding of Pore pressure of a formation is regarded as one of the major problems drillers face in the exploration area. This may be amongst others, the pressure acting on the fluids in the pore spaces of the rock. Pore pressure can be normal, abnormal or subnormal. Shear waves is a secondary wave that travels normal to the direction of propagation. Shear waves are slow and thus, get to the surface after primary wave. It is with this intrinsic property that this project was initiated and researched.

Data was obtained from a major operator in Niger Delta. Methods of this study are as follows: log description, interpretation and analysis and evaluation of pore pressure using the petro-physical parameters, model development using Domenico's equation as foundation and the shear wave velocity estimation.

The result from this study, shows the importance of well logs and shear wave velocity in the evaluation of pore pressure, it also indicates where pressure can be encountered during drilling activities.

Keywords : Shear wave, Pore pressure, Petrophysics, Wave velocity, Lithology, Density

INTRODUCTION

Sedimentation processes lead to deposition of various kinds of unconsolidated sediments in basins as formations. These newly deposited sediments are known for loosely packed, uncemented debris with high porosity and water content. As sedimentation persists in subsiding basins, the older sediments are progressively buried by younger sediments to increasingly greater depths. Consequently, pore spaces begin to reduce and fluids are trapped in certain spaces in the formation. These fluids include oil, gas, water, etc. They build a kind of pressure which they exert on the formation known as Pore pressure (Duffaut, 2011).

Pore pressure is defined as the pressure of the fluids in the pore spaces of the formation embedded in the earth. Formation fluids which include gases (nitrogen, sulphur, hydrogen sulphide, methane, etc.) and liquids (oil and water) contain pressure which increases with depth. The rate of the pressure increase (pore pressure gradient) depends on the fluid density in the pore spaces of the formation, which in

turn depends on the amount of dissolved materials (salt) in the fluid (Storvoll *et al.*, 2005). Thus, pressure in the pore spaces (pore pressure) is directly related to the fluid density in the pore spaces of the formation. According to Zhang (2011), pore pressure is by far one of the most valuable tools for drilling plan and for geomechanical and geological exploration. It varies from hydrostatic pressure. If the pressure in the formation is lower or higher than the hydrostatic pressure, it is abnormal. However, when the pore pressure is higher than the normal pressure, it is overpressure. (Zhang, 2011). The fundamental theory of pore pressure prediction can be linked to Terzaghi's and Biot's effective stress law (Biot, 1941; 1955; 1956; Terzaghi, 1996). The theory shows that pore pressure in the formation is an important variable for total stress and effective stress. The overburden stress, alongside the vertical stress and pore pressure can be expressed mathematically as in equation 1.

$$P_p = \frac{(\sigma_v - \sigma_e)}{\alpha} \dots \quad (1)$$

Where P_p = Pore pressure, σ_v = overburden stress, σ_e = vertical effective stress, α = Biot effective stress coefficient. It is assumed that $\alpha = 1$ in geopressure community. Prediction of pressure is mainly done by using time-migrated seismic data with well logs and geophysical data from local well. The method requires comprehensive analysis of velocity on the seismic data, conditioning of the well data, accompanied by calibration of the seismic data alongside the well values and forecasting of the pressure of the fluid on the kind of grid that was picked on the seismic log data. The final velocity is also calibrated by implementing well control and a velocity effective stress transform is estimated which honours the well and seismic data gotten from the control well locations. Overburden pressure for the area of prediction is estimated by integrating the data from the density log to extract a vertical stress versus depth relationship (Huffman, *et al.*, 2011).

This can be described mathematically as presented in equation 2.

$$\text{Vertical stress} = a \times z^b \dots \quad (2)$$

Where z = depth, a = coefficient and b = exponent Bowers (1995), equation (3) can then be used to make calibrations for velocity-effective stress. It is used for effectively predicting stress and predicting fluid pressure. The vertical and effective stress will then be correlated to

estimate the pore pressure using Terzaghi's basic relationship equation (Singh, 2010).

$$V = V_o + A^b \dots\dots\dots(3)$$

Where V= velocity obtained, V_o = stress velocity, A= a coefficient and B= an exponent

In compressive (P) waves, the medium vibrates in the direction that the wave is propagated, while in shear (S) waves, the ground vibrates transversely to the direction that the wave travels.

The velocity of shear waves tells us a lot about the properties and the shear strength of the material (Crice, 2002). If the velocities of P and S waves are known with the density of the materials in consideration, the elastic properties of the material that relates the magnitude of the strain response to the applied stress can be easily deduced. Known elastic properties include; Young modulus (E) which is the ratio of the applied stress of the fractional extension of the sample length parallel to the tension; Shear modulus (G) which is the ratio of the applied stress to the distortion of the plane originally perpendicular to the applied stress; Bulk modulus (K) which is the ratio of the confining pressure to the fraction reduction of the volume in response to hydrostatic pressure; Poisson ratio which is the ratio of the lateral strain to the longitudinal strain. They are presented in equations 4 – 7.

$$\text{Poisson ratio, } Fp = \frac{\left(\frac{V_p^2}{V_s^2}\right) - 2}{2\left(\frac{V_p^2}{V_s^2}\right) - 1} \dots\dots\dots(4)$$

$$\text{Shear modulus, } G = dVs^2 \dots\dots\dots(5)$$

$$\text{Young modulus, } E = 2G(1 + Fp) \dots\dots\dots(6)$$

$$\text{Bulk modulus, } K = \frac{1}{3} \left(\frac{E}{1 - 2Fp} \right) \dots\dots\dots(7)$$

Where V_p = compressive wave velocity, V_s =shear wave velocity, d=density and S= stress

Shear waves travel slower than the P-waves and this is imbedded in the complex wave train somewhere after the first arrival. In a normal refraction survey, identifying the P-wave is easy since they arrive first in the record. However, in a practical matter it is almost impossible to reliably pick a shear wave out of a normal refraction record (Duffaut *et al.*, 2011; Wair, *et al.*, 2012). Imbibing a seismic energy source that generates most shear waves and use of vibration sensors sensitive to shear waves is a potent remedy to this (multicomponent seismic) (Wair, *et al.*, 2012).

The aim of this study is to predict the pore pressure of a formation through shear wave sensitivities which is directly related to its velocity. Shear wave velocity increases with depth and effective pressure. Effective pressure is related to the difference between the confining pressure and pore pressure. Confining pressure is the pressure of the overlying rock column. Effective pressure increases with increase in confining pressure which leads to an increase in the velocity of the wave. The pore pressure may be hydrostatic if it is

connected to the surface which could be less or more hydrostatic. When the pore pressure is greater than hydrostatic, the effective pressure is reduced and the velocity is also reduced. In other words, pore pressure can be predicted with low shear wave velocities. Over pressured zones can be detected in a sedimentary sequence by their anomalously low velocities (Kao, 2010; Brahma, *et al.*, 2013; Wair, *et al.*, 2012), the response of this pore pressure is often seen in many velocity and density logs as an increase in their low frequency component with depth and causing them to experience some block character (Storvoll *et al.*, 2005).

Clays are more compactible than sandstone (Rieke, *et al.*, 1972; Uchida, 1984; Wolf and Chillingarian, 1975, Bowers 2002). The changes in the elastic properties (shear wave velocities) of formations are complex functions of both mechanical and chemical compaction process that predominate at different depths as a result of changes in the pore pressure and temperature (Kao, 2010; Brahma, *et al.*, 2013; Wair, *et al.*, 2012).

Terzaghi (1943) assumed that shear wave velocity increases with increase in differential stress. Differential stress is the subtraction of pore pressure from the overburden pressure. Experimentally, this can be proven by obtaining water saturated unconsolidated sand samples assuming near zero contact at low differential stress which means pore pressure is either high or kept constant while overburden is low or kept constant. Kao, (2010).

Shear waves must be significantly small compared to the cross sectional area of the medium which it is propagated, the velocity is equal to the square root of the ratio of the shear modulus (G), and a constant medium to density (ρ) of the medium as in equation 8.

$$v = \frac{\sqrt{G}}{\rho} \dots\dots\dots(8)$$

Two empirical correlations that are often used to relate shear wave velocity with pore pressure are Eaton's equation and Han and Batzle's correlation.

Eaton's equation

Eaton's (1975) equation is used to estimate pore pressures of different hole sections in a wellbore. It is often derived from stress and resistivity (both normal and measured resistivity values) and presented in equation 9 with Ebrom *et al.*, (2003) improvement (equation 10) that modified the equation and incorporated S-wave velocities from multicomponent seismic surveys.

$$P_p = S - (S - P_{hyd})(R - R_{log}) \dots\dots\dots(9)$$

Where P_p = Pore pressure, S = stress, P_{hyd} = hydrostatic pressure, R = normal resistivity, R_{log} = measured resistivity

$$\frac{\sigma_{eff.obv}}{\sigma_{eff.n}} = \left(\frac{V_{ps.obv}}{V_{ps.n}} \right)^{Esp} \dots\dots\dots(10)$$

Where $V_{ps.obv}$ = Interval velocities under abnormally pressured conditions, $V_{ps.n}$ = Interval velocities under normally pressured conditions, σ_n = effective stress under

normally pressured conditions, σ_{obv} = effective stress under abnormally pressured conditions

The velocities can be gotten using layer-stripping approach through the correlation of P-wave and S-wave data. This correlation is determined when seismic reflection is correctly flattened. However, this correlation can be gotten after computing a series of interval velocities of both the P-wave and S-wave (Kao, 2010; Brahma, *et al.*, 2013; Ferguson and Ebrom, 2008).

Han and Batzles' correlation (2004)

Han and Batzle opined that there is a linear correlation between shear wave velocity and compressional wave velocity shown in equation 11.

$$V_s = 0.79V_p - 0.79 \dots\dots\dots(11)$$

In a research study of the Milk River formation of the western Canadian sedimentary basin, V_s was estimated using a second poly-line equation presented in equation 12.

$$V_s = 0.000158V_p^2 - 0.62162 V_p + 2153.32 \dots\dots(12)$$

In a situation where porosity (ϕ) is included, equation (12) becomes equation 13.

$$V_s = 4.89 - 7.07\phi - 2.04 V_{cl} \dots\dots\dots(13)$$

V_{cl} and ϕ can be estimated from well logs

Study objectives are evaluation, quality control and correlation of log data in order to correct sonic log and compute porosity; Estimation of shear wave velocity using Domenico's shear wave and compressional wave velocity equation; Prediction of pore pressure by correlation of shear wave velocity and porosity.

According to Swarbrick (2002), the estimation of pore pressure uses the Terzaghi stress relationship between total

stress (vertical and horizontal compressive stress due to gravitational loading and sideways 'push', effective stress and the pore pressure in the simplified equation 14, (Kao, 2010; Nygaard, *et al.*, 2008; Sayers, *et al.*, 2002).

$$S = \sigma + P_p \dots\dots\dots(14)$$

Where S is the total stress, σ is the effective stress and P_p is the pore pressure. He continued by stating that the total vertical stress (S_v) is derived from the overburden, combined weight of the sediments and the contained fluids (Nygaard, *et al.*, 2008; Li, *et al.*, 2012; Bourgoynne, *et al.*, 1991; Ozkale 2006; Saul and Lumley, 2013).

METHODOLOGY

Data was generated from 5 wells (well36-3, well36-4, well36-6, well36-7 and well36-9) offshore Niger Delta operated by a major company. Figure 1 shows the location of the field and wells used.

EVALUATION OF POROSITY FROM LOG DATA

Porosity calculation is done by using Wyllie's equation/sonic (equation 15)

$$\phi = \frac{\Delta t_{log} - \Delta t_{ma}}{\Delta t_{fl} - \Delta t_{ma}} \dots\dots\dots(15)$$

Where Δt_{fl} = Transit time in pore fluid (depending on the depth), Δt_{ma} = Transit time in rock matrix and Δt_{log} = interval transit time from the log track.

Equation 15 is known as the time average equation, which is good for clean compacted formations with intergranular porosity containing fluids. Alternative methods employed the use of the total porosity log (denoted as PHIT) to get the data at each depth needed. This was used to validate porosities estimated from Wyllie's time average equation.

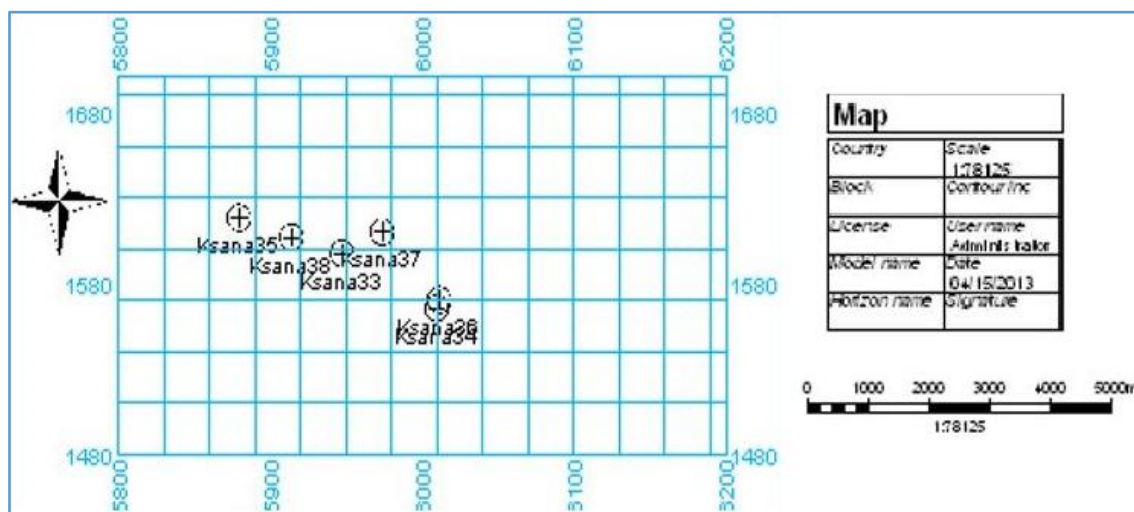


Figure 1: Location of the wells on the field

EVALUATION OF SHEAR WAVES USING POROSITY CALCULATED

This was done using a model developed by Domenico (1977), known as Domenico's shear wave and compressional wave velocity model. Equation 16 and 17 was the start up model with the assumptions that some elastic parameters are predicted from well logs and that the lithology has no structural elements (fault or fracture).

$$\frac{1}{V_p} = 0.163 + 0.365\phi \dots \dots \dots (16)$$

$$\frac{1}{V_s} = 0.224 + 0.889\phi \dots \dots \dots (17)$$

Where V_p = compressional wave velocity, V_s = shear wave velocity and ϕ = porosity

Next, Compressive wave can be determined from the inverse of sonic transit time for the log. Mathematically, this can be written as in equation 18.

$$V_p = \frac{1}{\Delta t_{log}} \dots \dots \dots (18)$$

Where V_p = compressional wave velocity (ft/s) and Δt_{log} = transit time (μ s/ft)

The shear wave velocity can then be computed from the compressional wave velocity by using Greenberg and Castagna (1992) model which is shown in equation 19 below. This is for sand beds while equation 20 serves for shale beds.

$$V_s = (0.80416V_p) - 0.85588 \dots \dots \dots (19)$$

$$V_s = (0.76969V_p) - 0.86735 \dots \dots \dots (20)$$

DERIVATION OF THE MODEL FOR PREDICTION OF PORE PRESSURE

Derivation of Pore pressure model begins with the use the drilling engineering model (Bourgoyne, *et al.*, 1991). This model relates pore pressure being proportional to density and height (depth). This is presented in equations 21-30.

$$P_o = 0.052 \times \rho_f \times h \dots \dots \dots (21)$$

$$\rho_f = \frac{\sqrt{G}}{V_s} \dots \dots \dots (22)$$

Substitute equation (22) into equation (21)

$$P_o = 0.052 \times \frac{\sqrt{G}}{V_s} \times h \dots \dots \dots (23)$$

$$\text{Where } G = \left(\frac{1-2\nu}{2\nu} \right) \lambda \dots \dots \dots (24)$$

$$\text{And } \lambda = \rho V_p^2 - 2\rho V_s^2 \dots \dots \dots (25)$$

Substitute equation (24) and equation (25) into equation (23)

$$P_o = \frac{0.052 \times \sqrt{\left(\frac{1-2\nu}{2\nu} \right) \rho V_p^2 - 2\rho V_s^2} \times h}{V_s} \dots \dots \dots (26)$$

$$\text{Where } \nu = \text{Poisson's ratio} = \frac{V_p^2 - 2V_s^2}{2(V_p^2 - V_s^2)} \dots \dots \dots (27)$$

Substitute equation (27) into equation (26) and collecting like terms and reducing to the lowest term will give equation 28.

$$P_o = \frac{0.052 \times \sqrt{1 + 2V_s^2 - V_p^2} \times h}{V_s} \dots \dots \dots (28)$$

$$\text{Where } V_p = 1.30V_s + 1.52 \dots \dots \dots (29)$$

Substitute equation (29) into equation (28) to give

$$P_o = \frac{0.052 \times \sqrt{1 + 2V_s^2 - (1.30V_s + 1.52)^2} \times h}{V_s} \dots \dots \dots (30)$$

Where P_o = Pore pressure (psig), V_s = shear wave velocity (ft/s) and h = depth (ft)

RESULTS AND DISCUSSIONS

Composite well logs which include gamma rays, resistivity, sonic, and total porosity logs of five wells (well36-3, well36-4, well36-6, well36-7, and well36-9) are correlated with depth as presented in Figures 2 – 6. Analysis, interpretation and result of well log data occurred under these categories; Lithology identification, Petrophysical analysis, Empirical correlation of parameters.

Lithology identification

On well 36-3, gamma ray log (track 3) shows the lithology is more of a sandstone formation based on the baseline picked for adequate discretization of the log track and was crossplot validated on track 7. The sonic log track (track 4) has high interval transit time (200 μ s/ft - 250 μ s/ft) at the beginning (zone 1) and decreased along in transition to zone 2. This indicates the time at which the acoustic wave travel in that formation is high due to the pore space within the grains of the formation, and indication that the formation is more of sandstone (Figure 2). The Gamma ray log of zone 2 has similar characteristics as zone 1. However, at the base of zone 2, there is a transition in the lithology from sandstone formation to shale formation. A corresponding sonic log (track 4) signature shows a decrease in the transit time of the acoustic wave velocity. This means an increase in velocity and a decrease in pore spaces with time. In zone 3, the gamma ray log signatures deflect to the right meaning the lithology is increasingly shale. The sonic log track has lower interval transit time. This means the time at which the acoustic wave travel in that formation is low due to lower amount of pore spaces in the formation filled with gas hydrocarbon.

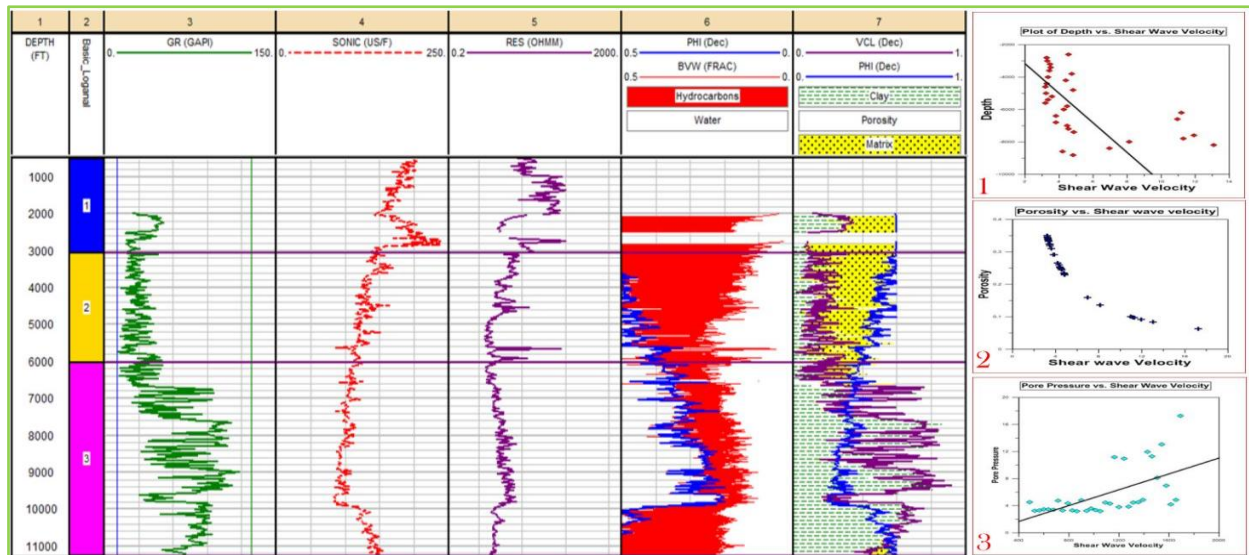


Figure 2: Well36-3 showing 7 tracks on the left. Crossplots of depth vs shear wave velocity (1), shear wave velocity and porosity for pore pressure prediction (2) and Pore Pressure against Shear wave velocity (3)

Gamma ray signature of well 36-4, (zone 1) starts with a higher left deflection (Figure 3). Based on the baseline picked, the deflection indicates that the lithology is more of an unconsolidated formation which is a sandstone formation. However, from 2000ft – 2700ft, the gamma ray log track (track 3) deflects to the right indicating the base of zone 1 is shale or compacted formation. Correlating this with sonic log track (track 4), there is more deflection to the right indicating velocity moving towards 200 μ s/ft. By implication, the formation at that depth is more porous and perhaps less consolidated. The presence of hydrocarbon is inferred from predominantly right resistivity logdeflection up to about 2000ft. Zone 2, boasts of blocky interlayered alternating formations. The resistivity log track has more deflection to

the left in zone 3, an indication of water zone. Gamma ray log of well 36-6 starts with a well indurated lithology. This shale constitutes zone 1. However, zone 2 and 3 have more of left deflection, meaning the formation at that zone is more of sandstone (Figure 4).

Correlating this with sonic log, a gradual left deflection occurs typifying a porous/fluid hosting formation. Resistivity log track had a higher deflection to the right from 2815ft – 3256.5ft (located in zone 2). This indicates the presence of little hydrocarbon validated by a high percentage of water saturation (87%). Well 36-7 has more unconsolidated formation; sandstone inferred from left gamma ray deflection(Figure5).

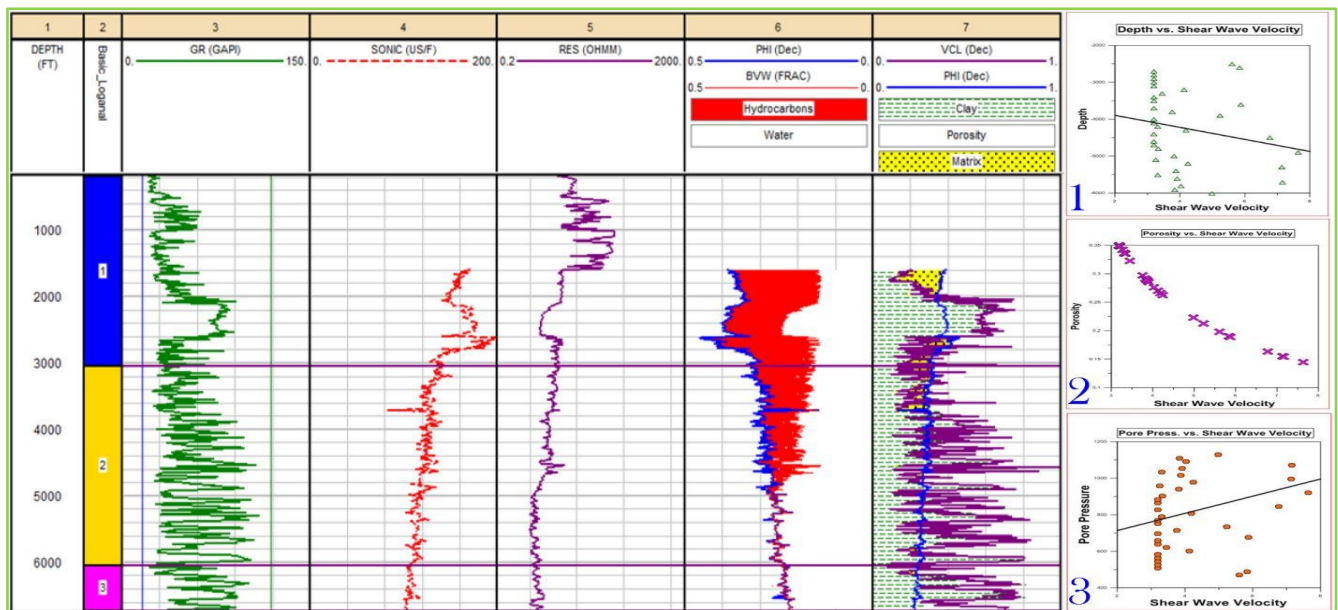


Figure 3: Well36-4 showing 7 tracks on the left. Crossplots of depth vs shear wave velocity (1), shear wave velocity and porosity for pore pressure prediction (2) and Pore Pressure against Shear wave velocity (3)

Sonic log signature is inconsistent, deflecting more to the right and slowly descending to the left due to the unconsolidated nature of the formation. The resistivity log of zone 1 deflects more to the right from 2713ft – 2945ft, an indication of hydrocarbon. From 3000ft -6000ft (zone 2), the resistivity log deflects mostly to the left; an indication of fresh water bearing zone (high conductivity). However, the latter part of zone 2 and all zone 3 (5000ft – 9000ft), the deflection on the gamma ray were mostly equal i.e. the formation region was made up of shale formation and sandstone formation based on the baseline picked. However, based on the deflection in the water saturation and porosity log, the formation in that zone is porous and fluid bearing. In

zone 1 of well 36-9, the gamma ray log showed more right deflection. From the baseline picked, that region is shale. From 3000ft – 4000ft (zone 2), there is more left deflections indicating that the formation in the zone is unconsolidated sandstone. From 4000ft – 6000ft (zone 2), the gamma ray signatures became equal, which means that zone is made up of both shale and sandstone formations (Figure 6). The sonic log track, on the other hand, had deflections that descended from the right to the left, meaning that the formation is mostly porous and unconsolidated. Sandstone is inferred. Right deflection on resistivity log is more prolific on zone 1 (2840ft – 3000ft). This is an indication of hydrocarbon at this depth.

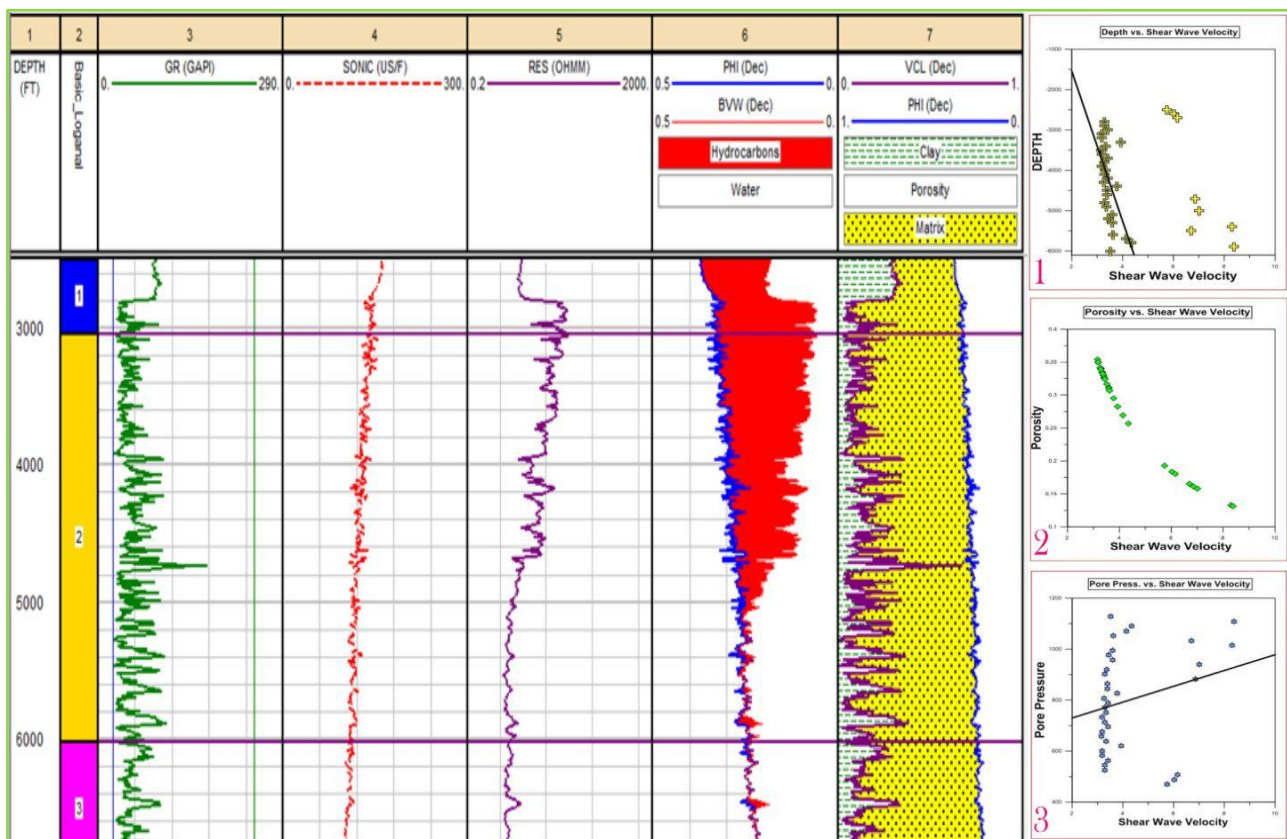


Figure 4: Well36-6 showing 7 tracks on the left. Crossplots of depth vs shear wave velocity (1), shear wave velocity and porosity for pore pressure prediction (2) and Pore Pressure against Shear wave velocity (3)

Petrophysical properties

Zone 1 of well 36-3 has higher resistivity showing that there is hydrocarbon in the pore spaces of the formation. The porosity log shows high deflection from zone 1 to zone 2. However, there is porosity drop in that it deflected to the left, meaning the formation (transition between zone 1 and 2) has low porosity and that the zone is unconsolidated. Water saturation log has some inference required for predicting the pore pressure. Where there is high resistivity (track 4), the water saturation is quite low; almost approaching zero (Figure2). Conversely, where there is low resistivity (track 4), the resultant water saturation is quite high almost approaching 1 (Figure2). It can therefore be inferred that water saturation is inversely proportional to resistivity. It can

also be inferred that in the porous zones of well 36-3, one of the fluids in the pore spaces is water which contributes to pore pressure in that formation.

The effective porosity computed for well 36-4 at zones 1 and 2 was high ranging from 0.15-0.35. This shows that the formation doesn't necessarily have many connected pores but probably many isolated pores due to the rapid sedimentation process typical of the shelf environment (Figure3). Water saturation in zone 1 is quite low (almost approaching zero) with a corresponding low hydrocarbon saturation index. However, in zone 2, water saturation was really high at almost 1. This shows that there are no hydrocarbons in that zone.

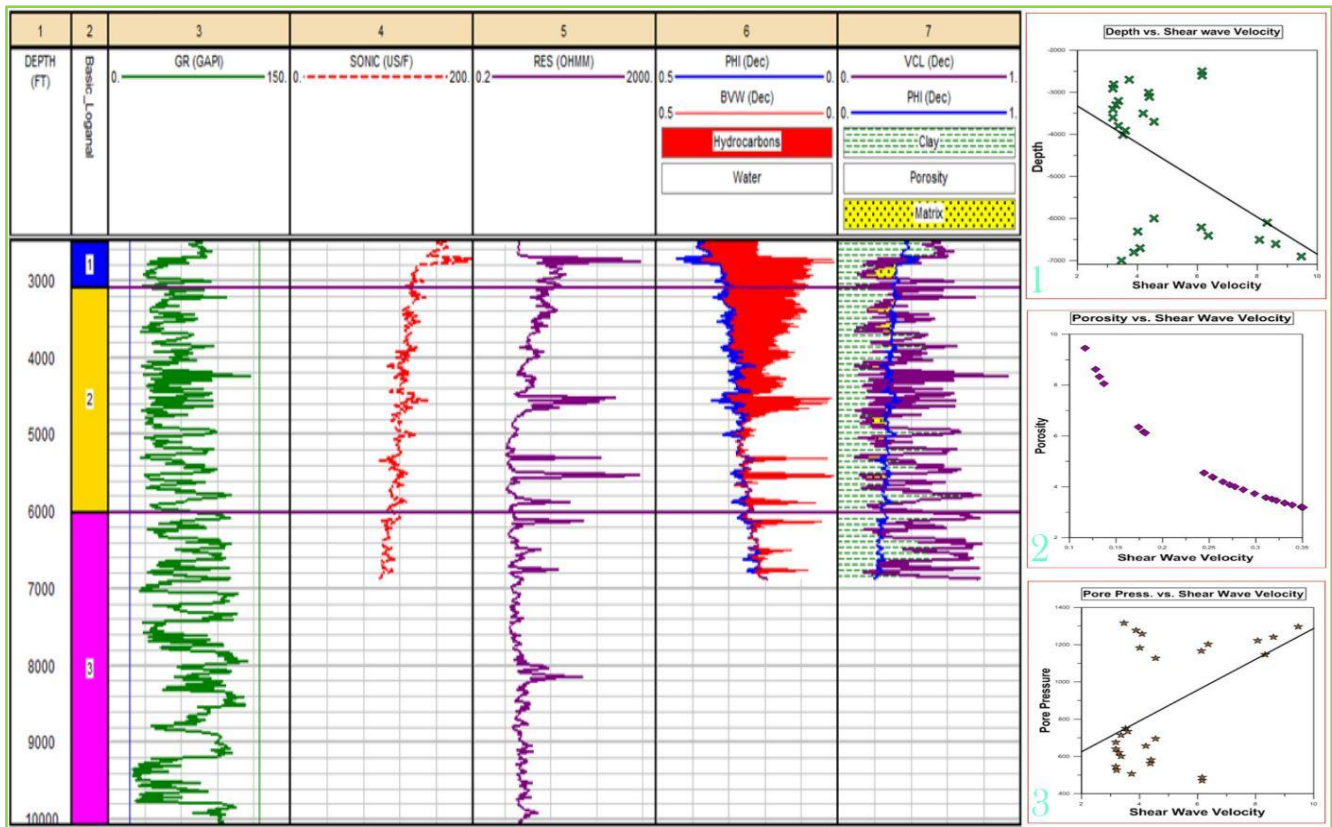


Figure 5: Well36-7 showing 7 tracks on the left. Crossplots of depth vs shear wave velocity (1), shear wave velocity and porosity for pore pressure prediction (2) and Pore Pressure against Shear wave velocity (3)

It also shows the zone is porous and water bearing. Average porosity value in zone 1 of well 36-6 is 0.19 making the lithology fairly porous compared to zone 2 with an average of 0.33. However, the formation is quite porous with little isolated pore spaces (Figure 4). Zone 1 is water bearing, but S_w decreases gradually to 0.7 in zone 2 (2900ft - 3230ft). This means that there is irreducible hydrocarbon fluid in that zone that may or may not be productive. Also from 3300ft - 7000ft, the water saturation increased back to 1 an indication of water bearing lithology.

From 2500ft - 4000ft (zone 2) of well 36-7, the porosity signatures were moderate and non-spurious. However, from 6000ft - 7000ft, this signature read low than the zone above it. This means that the zone between 2500ft - 4000ft is more porous than the zone between 6000ft - 7000ft. Zone 1, up to 2715ft is water bearing, but, S_w stands at an average value of 0.58 in zone 2, an indication of a resistive fluid likely hydrocarbon filling the pore spaces (Figure 5).

Average porosity in well 36-9 is 0.28. However, in zone 3, from 9000ft - 10000ft, porosity decreased to less than 0.1. This reduction portrays an increase in density and consolidation due to overburden pressure. Here water saturation reading is mostly approaching water filled scenarios at about 1. For depths between 2840ft - 3000ft, S_w is significantly less than (about 0.0682). It means the formation fluids existing at this shallow depth is hydrocarbon (Figure 6).

Estimation of Shear waves and Prediction of Pore pressure

Shear waves was estimated using the model derived from Domenico's shear wave velocity formula; equation 30. From the graph (Figure 2), between the first 6000ft, shear wave computed is quite low i.e. between 3 - 4.9m/s (Table 1). This means that the formation has large pore spaces fluid filled as seen in the resistivity log which could be methane gas (shallow methane gas). However, between 6200ft - 9000ft shear wave computed increased greatly from 4.2 m/s to about 17m/s meaning that the formation is highly compacted and consolidated. From the resistivity log, there is no much hydrocarbon and there are no much pore spaces in that particular zone of the formation.

From the function plot (Figure 3) between the first 4200ft in well 36-4, shear wave calculated is also low i.e. between 3 - 5.5ft/s, meaning that the formation is porous and contain fluid, likely gas (Table 2). However, between 4500ft - 5200ft shear wave computed rose to between 4 - 6ft/s, to terminate at 7ft/s at depth 5300ft. The inference drawn is porous and slightly resistive. Between 2500ft - 2800ft (zone 2) of well 36-6, the shear wave velocity is quite high in this shale formation (Table 3). Porosity log flags an average of 0.17 (Figure 4).

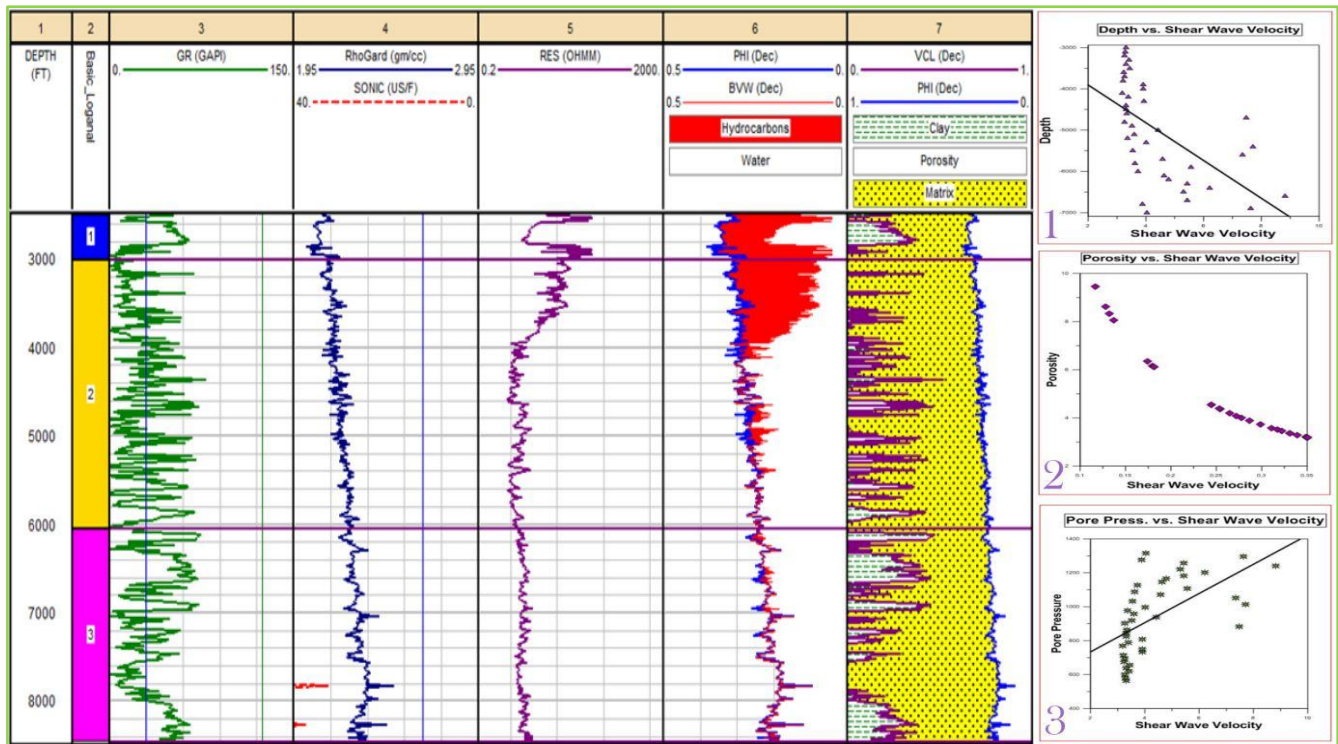


Figure 6: Well36-9 showing 7 tracks on the left. Crossplots of depth vs shear wave velocity (1), shear wave velocity and porosity for pore pressure prediction (2) and Pore Pressure against Shear wave velocity (3)

However, between the next 1600ft (zone 3) of well 36-7, the shear wave estimated in this location is low due to the unconsolidated nature of the formation (Table 4). This formation has average porosity of 0.19. On Table 4 and 5 (see appendix), the first 1500ft has shear wave velocity between 3ft/s – 6ft/s. It shows formation of this zone is appreciably porous at 20%(Figure5).

However, from 6000ft – 7000ft (zone 3), the shear wave velocity estimated rose from 3.4ft/s to climax at 8.33ft/s. This is an indication that formation of this zone has some compacted layers with reduced porosity due the spreading of the shear wave velocities calculated, meaning that some parts of that zone do not have pore spaces but most of that region is porous. The first 1700ft of well 36-9 from depth 3000ft, has low shear wave velocity at 3.5ft/s. This indicates that the formation in that zone is filled with pore spaces containing fluids (Figure6). However, from depth 6000ft – 7000ft, the shear wave rose to about 8ft/s (Table 6). This means that formation is made up of both compacted and unconsolidated formation. This also means the overall pattern of sedimentation is interbedded sandstone and shale.

Prediction of Pore pressure

Prediction of pore pressure was done using the model derived earlier (equation 30). The values computed for pore pressure estimates can be seen in Table 1 on the Appendix section. Correlation of porosity values at different depth, shear wave velocity and pore pressure is presented in Figures 2 – 6.

Pore Pressure Profiles (pressure gradient) of all wells

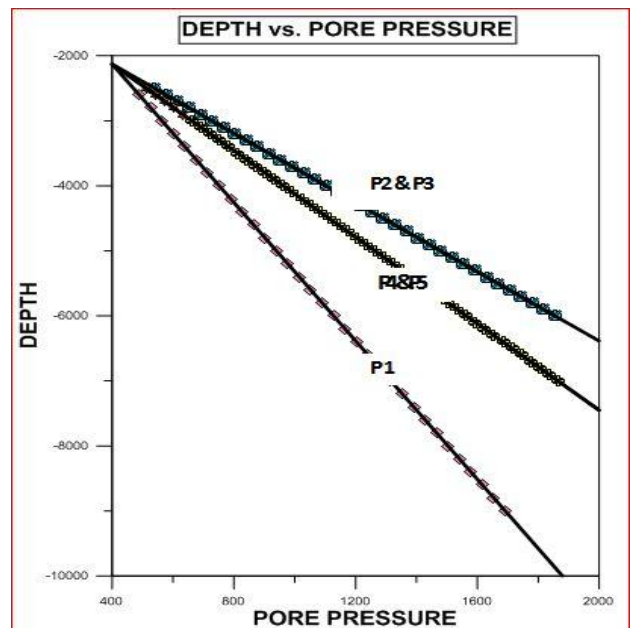


Figure 7: Function plot showing the pore pressure profile (pressure gradient) of all the 5 wells

From Figure7, all the pore pressure values/profiles of all 5 wells have some similarity: they increase with depth. However, pressure gradient curve in the most proximal well 36-3 designed as P1 has the least range of values of all the wells. In P1, the highest range of values is about 1700ps/sqft at depth 9000ft. Well 36-4 and 36-6 curves designated as P2

and P3 have similar values but have higher range of values than P1. As seen on Figure 4.21, P2 and P3 appears as a line because their values are similar, therefore P2 and P3 are overlapping. The highest range of values for P2 and P3 is about 1800lb/sqft at depth 6000ft. Well 36-7 and 36-9 with profiles P4 and P5 (overlapping) and most distal have the highest range of values of about 1900lb/sqft at depth 7000ft. The location of study wells affirms the variation observed to be that of increasing pressure with depth and distance away from shore. Well 36-3 being the most proximal has a value of 1700ps/sqft at 9000ft. This increased into the distal environment up to well 36-9 where pore pressure increased to 1900ps/sqft in a shallower depth.

Conclusion

From the previous chapter, which reports the analysis, results and discussion, it can be concluded that shear waves alongside porosity can be used for the determination of some important subsurface formation parameters, identification of hydrocarbon reservoirs and most of all, the degree of pore pressure in a particular well. The prediction of pore pressure before exploration is very vital as it provides the area at which the pressure encountered is normal, abnormal or subnormal. This information is very important for drillers, to avoid kick or blowout on the rig, if not maintained or controlled. The aim of the log plot was to identify and estimate the basic parameters needed to predict pore pressure. This includes the porosity, the lithology, the water saturation and the resistivity. The aim of the velocity – porosity graph is to correlate the shear wave velocity estimated and the porosity gotten from the log plot in order to forecast the degree of overpressure in a particular well by depth. In addition, it is also to know how productive and producible a reservoir is before it is drilled and completed.

Acknowledgement

The authors appreciate the support of MOST-CASTEP for research grant and workstation provided. The operator of the field case study is well appreciated for release of data and permissions. The inputs of anonymous reviewers are much appreciated.

References

1. **Biot, M., 1941.** "General theory of three-dimensional consolidation." *Journal of Applied Physics*, 12, 155–164.
2. **Biot, M., 1955.** "Theory of elasticity and consolidation for a porous anisotropic solid." *Journal of Applied Physics*, 26, 182–185.
3. **Biot, M., 1956.** "Theory of deformation of a porous viscoelastic anisotropic solid." *Journal of Applied Physics*, 27(5), 459–467.
4. **Bowers G.L., 1995.** Pore pressure estimation from velocity data: Accounting for overpressure mechanism besides undercompaction. SPE Drilling and Completions. Dallas USA.
5. **Bowers, G.L., 2002.** "Detecting high overpressure." *The Leading Edge*. Pp 174-177.
6. **Chilingarian G. V. and Wolf K. H., 1975.** *Compaction of Coarse-grained Sediments, Developments in Sedimentology 18* A. Elsevier Scientific Publishing Co., Amsterdam, Oxford, New York. ISBN 0 444 41152 6 pp., 233
7. **Bourgoyne A.T. (Jr), Millheim K.K., Chenevert M.E., Young F.S., (Jr.), 1991.** *Applied Drilling Engineering*, revised 2nd printing, pp. 246-250.
8. **Brahma Jwngsar, Sircar Anirbid, Karmakar G. P., 2013.** Pre-drill pore pressure prediction using seismic velocities data on flank and synclinal part of Atharamura anticline in the Eastern Tripura, India. *J Petrol Explor Prod Technol* (2013)3.Pp.93–103. DOI 10.1007/s13202-013-0055-0
9. **Crice Doug, 2002.** Borehole Shear-Wave Surveys for Engineering Site Investigations. *Geostuff*. <http://www.georadar.com/geostuff>. Pp.1-14.
10. **Domenico, S.N., 1977.** Elastic Properties of Unconsolidated porous sand reservoirs. *Geophysics*, 42(7).Pp.1339-1368.
11. **Duffaut K., 2011.** Stress sensitivity of elastic wave velocities in granular media. *Norgesteknikskaturvitenskapelige universitet 2011* (ISBN 978-82-471-2612-7) 102 s. Doktoravhandling ved NTNU (2011:45) NTNU.
12. **Duffaut, K., Avseth P., and Landro M., 2011.** Stress and Fluid Sensitivity in two North Sea oil fields-comparing Rock Physics models with Seismic observations. *The Leading Edge*, 30, pp 98 – 102.
13. **Eaton, B. A., 1975.** The equation for Geopressure prediction from well logs: SPE 5544.
14. **Ebrom, D., Heppard, P., Mueller, M., and Thomsen, L., 2003.** Pore pressure prediction from S - wave, C -wave, and P - wave velocities: SEG, Expanded Abstracts, 22, No. 1, 1370–1373.
15. **Ferguson R.J., and Ebrom D., 2008.** Overpressure prediction from PS seismic data. CREWES Research Report - Volume 20. Pp. 1-10.
16. **Greenberg, M., and Castagna, J., 1992.** Shear wave velocity estimation in porous rocks: Theoretical formulation, preliminary verification and applications. *Geophysical Prospecting*, 40. Pp.195-209
17. **Han De-hua, and Batzle Michael, 2004.** Estimate Shear Velocity Based on Dry P-wave and Shear Modulus Relationship. SEG Int'l Exposition and 74th Annual Meeting, Denver, Colorado. Pp. 1-4.
18. **Huffman, Meyer, Gruenwald, Buitrago, Suarez, Diaz, Mariamunoz and Dessay, 2011.** Recent Advances in Pore pressure Prediction in Complex Geologic Environment. *Onepetro. SPE-142211-MS*. <http://dx.doi.org/10.2118/142211-MS>. Pp. 8
19. **Kao, Jef C., 2010.** Estimating Pore Pressure Using Compressional and Shear wave Data From Multicomponent Seismic Nodes in Atlantis Field, Deepwater Gulf of Mexico. 2010 SEG Annual Meeting, Colorado.

20. **Li Shuling, Jeff George and Cary Purdy, 2012.** Pore-Pressure and Wellbore-Stability Prediction to Increase Drilling Efficiency. Society of Petroleum Engineers. OnePetro. <http://dx.doi.org/10.2118/144717-JPT>
21. **NygaardRunar, MojtabaKarimi, GeirHareland, and Hugh B. Munro, 2008.** Pore-Pressure Prediction in Overconsolidated Shales. Society of Petroleum Engineers. OnePetro. DOI - <http://dx.doi.org/10.2118/116619-MS>
22. **OzkaleAslihan, 2006.** Overpressure prediction by mean total stress estimate using well logs for compressional environments with strike – slip or reserve faulting stress state. Unpublished Master's Thesis, TAMU. Pp 172
23. **Rieke, H. H., Chillinger, G. V. and Mannon, R. W., 1972.** Application of petrography and statistics to the study of some petrophysical properties of carbonate reservoir rocks. In G. Chillinger et al., eds., Oil and gas production from carbonate rocks, p. 340- 354, Elsevier.
24. **Singh, Y. R., Metilda Pereira, R. K. Srivastava, P. K. Paul, and R. Dasgupta, 2010.** Regional Pressure Compartmentalisation Preview using Pore Pressure Approach - A Case study from NE India. SEG Technical Program Expanded Abstracts 2010: pp. 2217-2220. doi: 10.1190/1.3513288.
25. **Storvoll, V., K. Bjørlykke, and N. H. Mondol, 2005.** Velocity-depth trends in Mesozoic and Cenozoic sediments from the Norwegian Shelf: AAPG Bulletin, v. 89, p. 359 – 381.
26. **Swarbrick, R.E., 2002.** "Challenges of Porosity-Based Pore Pressure Prediction," CSEG Recorder. Issue 75.
27. **Sayers C. M., Johnson, G. M., and Denyer G., 2002.** Predrill pore-pressure prediction using seismic data. GEOPHYSICS, Vol. 67, No. 4. Pp. 1286-1292
28. **Saul, M., and Lumley, D., 2013.** A new velocity-pressure-compaction model for uncemented sediments. Geophysical Journal International, 193. Pp. 905-913.
29. **Terzaghi, 1943, 1996. Terzaghi Karl, 1943.** Theoretical Soil Mechanics. John Wiley & Sons, Inc. Pp. 526
30. **Uchida T., 1984.** Properties of Pore Systems and their Pore-Size Distributions in Reservoir Rocks. Journal of the Japanese Association for Petroleum Technology. Vol.49, no. 1.
31. **Wair, B.R., DeJong, J.T and Shantz, T., 2012.** Guidelines for Estimation of Shear Wave Velocity Profiles. PEER Report 2012/08. Pacific Earthquake Engineering Research Center Headquarters at the University of California. Pp. 95.
32. **Zhang Jincai, 2011.** Pore pressure prediction from well logs: methods, modifications and new approaches. Earth Science Reviews. Doi: 10.1016/j.earscirev.2011.06.001. Vol. 108. Pp. 50 – 63.

Appendix

Table 1:Depth, porosity and estimated shear waves for well 36-3

DEPTH (FT)	POROSITY(FRAC)	SHEAR WAVES (FT/S)	PORE PRESSURE (PSIG)
-2600	0.2447	4.550039745	488.6876892
-2800	0.3419	3.265955581	526.2790499
-3000	0.3382	3.30142179	563.8704106
-3200	0.3234	3.451339223	601.4617714
-3400	0.3194	3.494223699	639.0531321
-3600	0.3247	3.437627514	676.6444928
-3800	0.2349	4.737852265	714.2358535
-4000	0.335	3.332722334	751.8272142
-4200	0.254	4.385080203	789.4185749
-4400	0.34	3.28407225	827.0099356
-4600	0.35	3.190912282	864.6012963
-4800	0.2311	4.814916998	902.192657
-5000	0.3459	3.22846108	939.7840177
-5200	0.31	3.599323327	977.3753784
-5400	0.3317	3.365628785	1014.966739
-5600	0.35	3.190912282	1052.5581
-5800	0.2496	4.461608749	1090.149461
-6000	0.26	4.284857314	1127.740821
-6200	0.0981	11.17931737	1165.332182
-6400	0.2915	3.825796196	1202.923543
-6600	0.1	10.97213079	1240.514903
-6800	0.291	3.832313299	1278.106264
-7000	0.2482	4.486522039	1315.697625
-7200	0.245	4.544524984	1353.288986
-7400	0.2296	4.846031875	1390.880346
-7600	0.0917	11.93868768	1428.471707
-7800	0.097	11.30288337	1466.063068
-8000	0.1363	8.103025102	1503.654428
-8200	0.0835	13.07676716	1541.245789
-8400	0.1592	6.955612066	1578.83715
-8600	0.2654	4.198494756	1616.428511
-8800	0.2301	4.835615663	1654.019871
-9000	0.0627	17.24723742	1691.611232

Table 2: Depth, porosity and estimated shear waves for well 36-4

DEPTH (FT)	POROSITY (FRAC)	SHEAR WAVE VELOCITY (FT/S)	PORE PRESSURE (PSIG)
-2500	0.1979	5.612519511	469.8920089
-2600	0.1903	5.83373732	488.6876892
-2700	0.3497	3.193630113	507.4833696
-2800	0.3483	3.206374786	526.2790499
-2900	0.35	3.190912282	545.0747303
-3000	0.35	3.190912282	563.8704106
-3100	0.35	3.190912282	582.666091
-3200	0.2702	4.124599192	601.4617714
-3300	0.323	3.455580244	620.2574517
-3400	0.3486	3.203635229	639.0531321
-3500	0.35	3.190912282	657.8488124
-3600	0.189	5.873335644	676.6444928
-3700	0.35	3.190912282	695.4401731
-3800	0.2972	3.753038084	714.2358535
-3900	0.2125	5.231425171	733.0315338
-4000	0.35	3.190912282	751.8272142
-4100	0.35	3.190912282	770.6228945
-4200	0.337	3.313090351	789.4185749
-4300	0.2663	4.184438325	808.2142553
-4400	0.35	3.190912282	827.0099356
-4500	0.1636	6.771379276	845.805616
-4600	0.35	3.190912282	864.6012963
-4700	0.35	3.190912282	883.3969767
-4800	0.3355	3.327792559	902.192657
-4900	0.1447	7.640686042	920.9883374
-5000	0.2918	3.821896563	939.7840177
-5100	0.3422	3.26311331	958.5796981
-5200	0.2628	4.239637901	977.3753784
-5300	0.1553	7.127497386	996.1710588
-5400	0.288	3.871887003	1014.966739
-5500	0.3363	3.319935182	1033.76242
-5600	0.2853	3.908208684	1052.5581
-5700	0.1546	7.15925183	1071.35378
-5800	0.2764	4.032915039	1090.149461
-5900	0.2899	3.846729376	1108.945141
-6000	0.2229	4.990067271	1127.740821

Table 3: Depth, porosity and shear wave velocity for well 36-6

DEPTH (FT)	POROSITY (FRAC)	SHEAR WAVE VELOCITY (FT/S)	PORE PRESSURE (PSIG)
-2500	0.1979	5.612519511	469.8920089
-2600	0.1903	5.83373732	488.6876892
-2700	0.3497	3.193630113	507.4833696
-2800	0.3483	3.206374786	526.2790499
-2900	0.35	3.190912282	545.0747303
-3000	0.35	3.190912282	563.8704106
-3100	0.35	3.190912282	582.666091
-3200	0.2702	4.124599192	601.4617714
-3300	0.323	3.455580244	620.2574517
-3400	0.3486	3.203635229	639.0531321
-3500	0.35	3.190912282	657.8488124
-3600	0.189	5.873335644	676.6444928
-3700	0.35	3.190912282	695.4401731
-3800	0.2972	3.753038084	714.2358535
-3900	0.2125	5.231425171	733.0315338
-4000	0.35	3.190912282	751.8272142
-4100	0.35	3.190912282	770.6228945
-4200	0.337	3.313090351	789.4185749
-4300	0.2663	4.184438325	808.2142553
-4400	0.35	3.190912282	827.0099356
-4500	0.1636	6.771379276	845.805616
-4600	0.35	3.190912282	864.6012963
-4700	0.35	3.190912282	883.3969767
-4800	0.3355	3.327792559	902.192657
-4900	0.1447	7.640686042	920.9883374
-5000	0.2918	3.821896563	939.7840177
-5100	0.3422	3.26311331	958.5796981
-5200	0.2628	4.239637901	977.3753784
-5300	0.1553	7.127497386	996.1710588
-5400	0.288	3.871887003	1014.966739
-5500	0.3363	3.319935182	1033.76242
-5600	0.2853	3.908208684	1052.5581
-5700	0.1546	7.15925183	1071.35378
-5800	0.2764	4.032915039	1090.149461
-5900	0.2899	3.846729376	1108.945141
-6000	0.2229	4.990067271	1127.740821

Table 4: Depth, porosity and estimated shear wave velocity between 2500ft – 4000ftfor well 36-7

DEPTH (FT)	POROSITY (FRAC)	SHEAR WAVE VELOCITY (FT/S)	PORE PRESSURE (PSIG)
-2500	0.18	6.162948354	469.8920089
-2600	0.18	6.162948354	488.6876892
-2700	0.299	3.73063335	507.4833696
-2800	0.3484	3.20546108	526.2790499
-2900	0.35	3.190912282	545.0747303
-3000	0.2544	4.378253042	563.8704106
-3100	0.253	4.402241621	582.666091
-3200	0.3308	3.374716355	601.4617714
-3300	0.3391	3.292724166	620.2574517
-3400	0.35	3.190912282	639.0531321
-3500	0.265	4.204772417	657.8488124
-3600	0.35	3.190912282	676.6444928
-3700	0.2446	4.551880974	695.4401731
-3800	0.3314	3.368652532	714.2358535
-3900	0.3107	3.591279368	733.0315338
-4000	0.3172	3.518267549	751.8272142

Table 5: Depth, porosity and estimated shear wave velocity between 6000ft – 7000ftfor well 36-7

DEPTH (FT)	POROSITY (FRAC)	SHEAR WAVE VELOCITY (FT/S)	PORE PRESSURE (PSIG)
-6000	0.2449	4.546361751	1127.740821
-6100	0.1324	8.337251842	1146.536502
-6200	0.1811	6.12602833	1165.332182
-6300	0.2777	4.01420547	1184.127862
-6400	0.1745	6.354431104	1202.923543
-6500	0.1368	8.073944413	1221.719223
-6600	0.1279	8.624920327	1240.514903
-6700	0.2721	4.096062496	1259.310584
-6800	0.2866	3.890635784	1278.106264
-6900	0.1164	9.458983954	1296.901944
-7000	0.3223	3.463027164	1315.697625

Table 6: Depth, porosity and shear wave velocity for well 36-7

DEPTH (FT)	POROSITY (FRAC)	SHEAR WAVE VELOCITY (FT/S)	PORE PRESSURE (PSIG)
-3000	0.3377	3.306273687	563.8704106
-3100	0.3398	3.285990966	582.666091
-3200	0.3425	3.260275982	601.4617714
-3300	0.3256	3.428198441	620.2574517
-3400	0.3373	3.310165485	639.0531321
-3500	0.3243	3.441834883	657.8488124
-3600	0.3449	3.237753763	676.6444928
-3700	0.3413	3.271655003	695.4401731
-3800	0.3476	3.212785344	714.2358535
-3900	0.2853	3.908208684	733.0315338
-4000	0.2854	3.906851289	751.8272142
-4100	0.35	3.190912282	770.6228945
-4200	0.3284	3.399191536	789.4185749
-4300	0.2844	3.920467822	808.2142553
-4400	0.3381	3.30239103	827.0099356
-4500	0.3383	3.300453119	845.805616
-4600	0.3332	3.350591111	864.6012963
-4700	0.1479	7.478139529	883.3969767
-4800	0.3418	3.266904105	902.192657
-4900	0.3174	3.51606808	920.9883374
-5000	0.2519	4.421274998	939.7840177
-5100	0.3091	3.609718662	958.5796981
-5200	0.3323	3.359597547	977.3753784
-5300	0.2776	4.015638503	996.1710588
-5400	0.1432	7.719337249	1014.966739
-5500	0.3138	3.556084069	1033.76242
-5600	0.1504	7.35588353	1052.5581
-5700	0.2434	4.574092523	1071.35378
-5800	0.309	3.610877407	1090.149461
-5900	0.1997	5.562561292	1108.945141
-6000	0.2983	3.739314442	1127.740821
-6100	0.2399	4.640132225	1146.536502
-6200	0.2322	4.792352173	1165.332182
-6300	0.2046	5.430963225	1184.127862
-6400	0.1785	6.214016958	1202.923543
-6500	0.2094	5.307951417	1221.719223
-6600	0.1251	8.814152709	1240.514903
-6700	0.2041	5.44410564	1259.310584
-6800	0.2864	3.893329014	1278.106264
-6900	0.1447	7.640686042	1296.901944
-7000	0.2753	4.048882974	1315.697625